Modified PSO-Based Virtual Inertia Controller for Optimal Frequency Regulation of Micro-Grid

[1]M. Hamza, [2]M. Buhari, & [3]A. A. Sadiq.

[1]Department of Electrical Engineering, Ahmadu Bello University Zaria, Nigeria.
[2]Department of Electrical Engineering, Bayero University, Kano, Nigeria.
[3]Department of Electrical and Electronics Engineering, Federal University of Technology, Minna. Nigeria.
: ahmad.abubakar@futminna.edu.ng; +(234) 805-787-9333

Received:04.09.2022 **Accepted**:29.11.2022 **Published**:29.11.2022

Abstract:
Owing to the growing need to address the energy crisis by the traditional sources (e.g. Thermal power plants), as well as the associated environmental concerns posed, the power system witnessed increased penetration of power electronics-based power sources like solar, wind, and energy storage in terms of battery technologies. Consequently, modern compared with traditional power systems have become more susceptible to large frequency fluctuations due to the emergence of stability issues. Prominent among these include the reduction of system properties such as damping and inertia which are significant characteristics of system stability. Insufficient inertia drives the grid frequency outside the acceptable range under severe disturbances and this may lead to an outage of generators and tripping, unscheduled shedding of load, system collapse, and in the severe scenario, an entire power blackout, this threatens the system dynamic security. To preserve the system's dynamic security, this paper proposes an alternative approach to frequency regulation built upon a PID-based Virtual Inertia Control (VIC) which imitates the inertia property. The proposed virtual inertia uses the frequency derivative to emulate virtual inertia. The optimality search capability of the Particle Swarm Optimization (PSO) technique is used to design the proposed controller. Evaluation of the robustness of the proposed controller is demonstrated through Time Domain Analysis, considering different system operating ranges for improving frequency stability and resilience. Improved performance of the proposed controller when paralleled with the traditional virtual inertia controller shows a 69.2% reduction in frequency nadir under the condition of reduced system inertia, 70% without RESs integration. Also, 50.7% and 44.4% improvement in the reduction of frequency nadir and maximum overshoot respectively were observed under the situation of nominal system inertia, 100%, and Renewable Energy Systems (RESs) penetration.

Keywords: **Distributed Generation (DG), Frequency stability, Virtual inertia, Particle Swarm Optimization (PSO), Micro-Grid.**

1. Introduction

IN recent years, Renewable Energy Sources (RES) in the form of Distributed Generators (DG) are gaining favorable penetration into the power system, this is majorly due to growing concerns for conservational issues, the energy crisis, and the growth of the economy. Aside from the emergence of Micro-Grids (MG), RES/DGs penetration also displaces several conventional generators that contribute to the reserve power and inertial response for frequency control. This drastically reduces the entire system's inertial (H) responses as well as damping (D) effects usually during 1-10s cycles in the operation. As a result, the frequency variations of MG escalate, which further causes greater frequency deviations at the expense of system stability and resiliency, eventually leading to cascading failure or power blackout. In addition, the RES type of generators often has low inertia which can be non-existent owing to the use of power electronics as an interface without rotating mass. Consequently, RES types generators often do not participate in the control of frequency during normal operation. [1]. Thus, dynamic security of the modern power system characterized by low system damping effect and inertia due to RESs penetration is a major concern for the present and future power system planning, design, operation, and control. This is because of the reduction in the overall stability margin.

In addressing the stability concerns and problems posed by the power electronic-based RES generation, one straightforward solution is the operations of a greater number of synchronous generators. This will ensure the provision of adequate spinning reserve and system inertia [2]. The major drawback of the aforementioned approach is seen when some of the synchronous generators operate at their minimum allowable level, which reduces efficiency. The operation of synchronous and conventional generators is also associated with emissions and increases in the prices of energy.

In enhancing system inertia, the withstand capability requirements defined by RoCoF, or simply called Rate of Change of Frequency, by synchronous generators were changed in [3]. Though this solution approach is considered efficient and suitable by operators, as stated in [4], the associated costs involved due to the testing of the generator is a major limitation to its acceptance and applications. Moreover, the approach ignores inertia enhancement. PV power curtailments to regulate frequency or inertia synthesis have been suggested in [5-7]. However, this approach is simply practicable in PV-dominated systems, like those of the California power network which is already implementing active power curtailment policies [7]. Aside from this, an opportunity cost considered to be non-trial

in the wasted energy would hinder the wide adoption of such an approach, because inverters of the PV are functioning often beneath the Maximum Power Points (MPPs). Another approach for inertia enhancement is employing synchronous condensers – synchronous generators – without prime movers or demanded loads [8]. Nonetheless, the associated huge operating and capital costs have hindered their application in inertia enhancement.

Turbines of Wind generators have rotating masses with associated kinetic energy similar to synchronous generators. But unlike synchronous generators, the rotating speeds of wind turbines are often separated from the grid frequency using power electronic converters for optimal control of speed to achieve the highest energy harvesting [9], [10]. As a result, wind generation systems classified as variable-speed systems naturally provide no inertia to the power grid. In using the kinetic energy stored in the turbines of wind generators, the grid-injected power (or electromagnetic torque) can be modified in accordance to the grid frequency at times of contingencies [10]. Using this method, the virtual inertia can be emulated by such types of wind turbines. Considering inertia synthesis, the rate of change of frequency is proportionally linked to the electromagnetic torque (i.e., df/dt) [11]. Several approaches for modifying the control of virtual inertia for different wind turbines are documented in [12−14]. However, the wind turbines should be able to recover their rotor speeds after producing the virtual inertia response. But this can be a significant issue [15]. As analyzed and evaluated by [9] and [16], the processes for recovering the rotor speed will drastically modify the wind turbines' inertia response and may result in rotor stall arising frequency dip. As substantiated by the response of the wind inertial in Hydro-Quebec, the synthesized inertia of wind turbines is still not identical in practice tests to synchronous inertia [3]. For speed recovery, numerous nonlinear-based inertia control techniques for accurate inertia synthesis by wind turbines enabling easy and fast transitions between inertial response mode and MPP tracking mode were suggested in [17−21].

The innovative approach is to emulate the dynamic behavior of the synchronous generator in the power system in enhancing the system inertia. This innovative approach is called Virtual Synchronous Machine (VISMA) [22-24], Virtual Synchronous Generator (VSG) [25, 26], or Synchronverter [27-29] which imitates the activity of the prime mover during disturbances to enhance the frequency stability. The virtual inertia control scheme is a crucial part of the VSG. It is realized by using an energy storage system (ESS), a power electronic inverter, and then a proper control technique is employed to determine the required inertia output power for the enhancement of the system inertia and frequency stability.

Recently, the strategy for the control of virtual inertia through emulation has received a lot of attention from researchers [26, 30]. Hence, depending on the control objectives, there are several types of virtual control techniques of inertia. However, the derivative of frequency technique expressed df/dt , virtual inertia control provides an effective solution for emulating virtual inertia power to enhance the stability of frequency and system inertia [31-33]. However, in [31-33], the inertia constants, a significant factor used to emulate extra inertia into the system is a fixed value. But the improper selection of this fixed value causes greater frequency excursion, slow time to recovery, and eventual instability.

Hence, an advanced control technology is required to provide an optimal virtual inertia constant. The Model Predictive Control (MPC) for the inertia power synthesis in a derivative technique-based approach was proposed in [34]. Although the predictive control-based strategy in [34] has the advantages of straightforward structure and fast response, it requires more time for each sampling time calculation. In [35], a robust theory combined with virtual inertia control results in r frequency oscillation mitigation in the high RESs penetration scenarios. In [36], an approach based on the H_infinite technique of the robust virtual inertia control is proposed to analyze the islanded MG frequency stability in the presence of high levels of RESs. The fuzzy logic control is proposed in [37, 38] for the synthesis of virtual inertia to support the frequency stability of the islanded μGs.

Although a good dynamic response was obtained from the control techniques [35-38], they have various shortcomings such as their dependence on the experience of the designer and the need for a longer time required for computation. However, the proportional–integral–derivative (PID) is commonly deployed in the study of frequency control problems. This is attributed to its low cost and simplicity. In addition, it provides a reliable result under contingencies and variations in system operational parameters such as system uncertainties. Hence, in this study, a proportional-integral-derivative (PID) controller is employed to obtain the optimal values of virtual inertia constant for operational inertia emulation thereby enhancing the system frequency stability.

I. Inertia Constant Effect in Regards to Frequency Regulation

The problem of frequency stability arising from the mismatch between generated power and load demand is a challenging task in the micro-grid design and operation. In the traditional synchronous generator-dominated power network, the damping effects and inertia properties obtained from the rotor are critical in frequency stability regulation during the disturbances. The swing equation (1) expresses the relationship between generated power, system inertia, load power, system damping, and frequency excursion [39].

$$\Delta P_m - \Delta P_L = 2H_s(\Delta f) + D(\Delta f) \tag{1}$$

Where f is the system frequency, Δf is the system frequency deviation, ΔP_m is the change in the generated power from the synchronous generator, ΔP_L is the change in the load power, and H and D are the inertia and the damping property of the system.

For the modern power system penetrated by DGs/RESs, the converter control response replaces the natural response due to the generator's rotating mass (natural inertia compensation).

However, the response due to the control of the converter is comparatively slow compared to the natural response of the rotating mass. This result in a lack of high inertia power compensation immediately from 1 to 10s, especially after a contingency. The main and subordinate controls in place are not robust to neutralize the disturbances in the scenarios with low system inertia and damping which result from increased penetration of RES. This leads to an excessive RoCoF, resulting in rapid deviations in frequency. Equation (2) expresses the inertia constant relations of between traditional synchronous generators and MG [39].

$$H = \sum_{i}^{n} (H_{SGi} S_{SGI}) \Big/ S_{MG} \tag{2}$$

Where S_{GS} and S_{MG} are the synchronous generator-rated power and the micro-grid's total power.

turbine system. The transients of the generator as well as the exciter and their corresponding effects can be ignored since it is considered considerably faster [66]. In this study, the frequency response model shown in Fig. 2 is employed as the test system representing the studied MG shown in Fig. 1. Since the RESs-based generations (solar and wind power) and the load provides no frequency regulation, they may be seen as a form of disturbances to the MG. Mainly, three units – inertia control, main control, and subordinate control – are deployed for the improvement of the system's frequency stability after the occurrence of a disturbance. The inertia provided by the ESS-based inertia control neutralizes the mismatched power at 1-10s. The main control unit, in this case, the governor system helps to stabilize the frequency to another value in steady-state in 10-30s. The subordinate control will recover the system frequency to its nominal value within 10-30 minutes especially

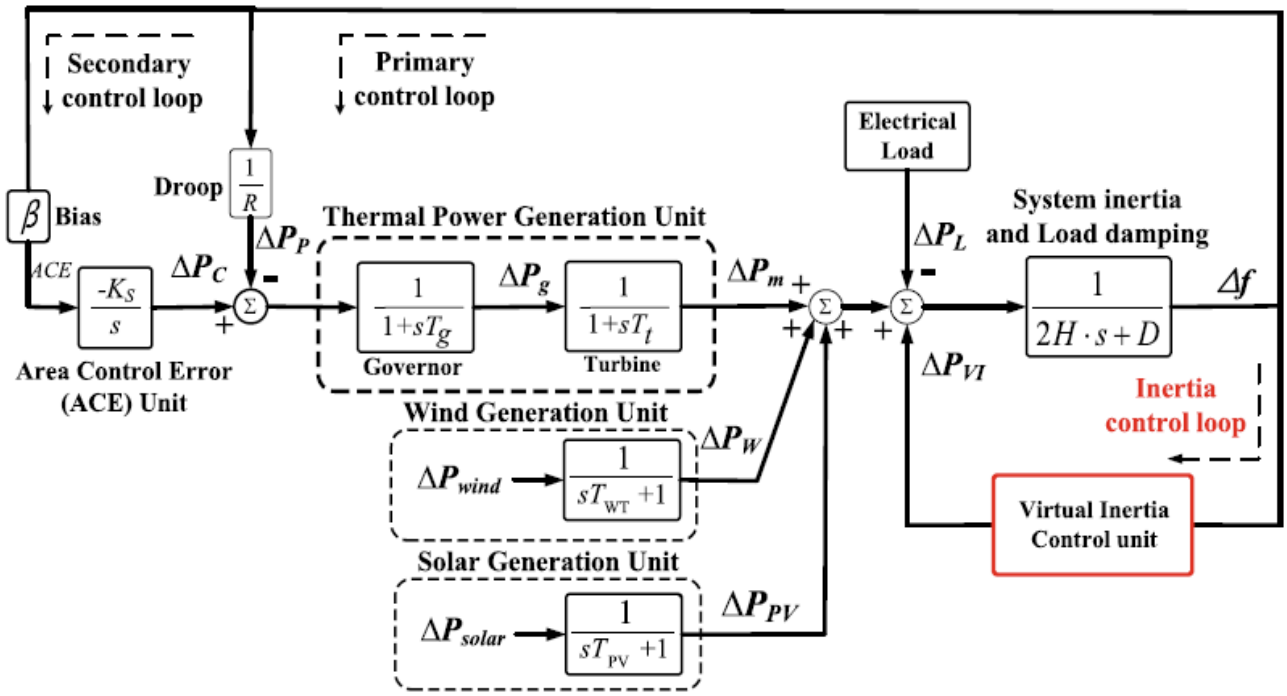

Fig. 1. Dynamic frequency response model of the test power system with different control schemes

TABLE I
THE MICRO-GRID DYNAMIC PARAMETERS

Parameter	Value	Parameter	Value
D (p.u./Hz)	0.0160	J_{VI} (p.u.s)	0.6
H (p.u.s)	0.0830	R (Hz/p.u)	2.6
T_g (s)	0.07	β (p.u./Hz)	0.98
T_t (s)	0.03	T_{ESS}(s)	1.0
T_W(s)	1.4	T_{PV}(s)	1.0

II. SYSTEM CONFIGURATION

In remote power systems networks, frequency dynamics are mainly caused by the dynamics of the rotor and governor-

Relevant model parameters are presented in Table I. Considering the dynamic effects of generations and load including inertia, primary, and secondary control (from Fig. 1),

when it is based on area control error (ACE). Based on [39], the MG's simplified model under study – with a low-order dynamic model – as depicted in Fig. 2 is considered adequate for the study and analysis of frequency stability. In addition, [40] studied frequency responses obtained both with the simplified and detailed model of MG. A reasonably accurate result was observed with the simplified model under changing conditions. Hence, the simple model employed herein is adequate and precise for the scope of frequency stability in this paper. Equations (4) to (8) describes the models of the MG adopted.

the system frequency deviation is obtained and given by the equation (3):

$$\Delta f(s) = \frac{1}{2Hs + D} (\Delta P_m + \Delta P_W + \Delta P_{PV} + \Delta P_{inertia} - \Delta P_L) \tag{3}$$

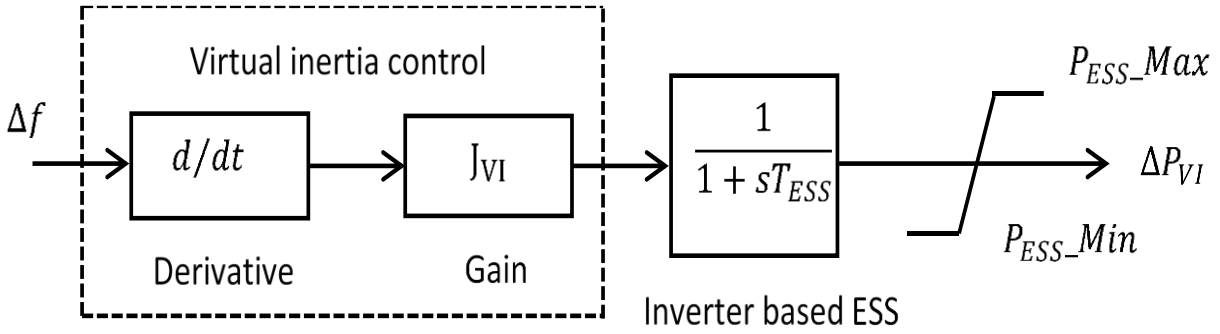

Fig. 2. Conventional Virtual Inertia Control (C-VIC)

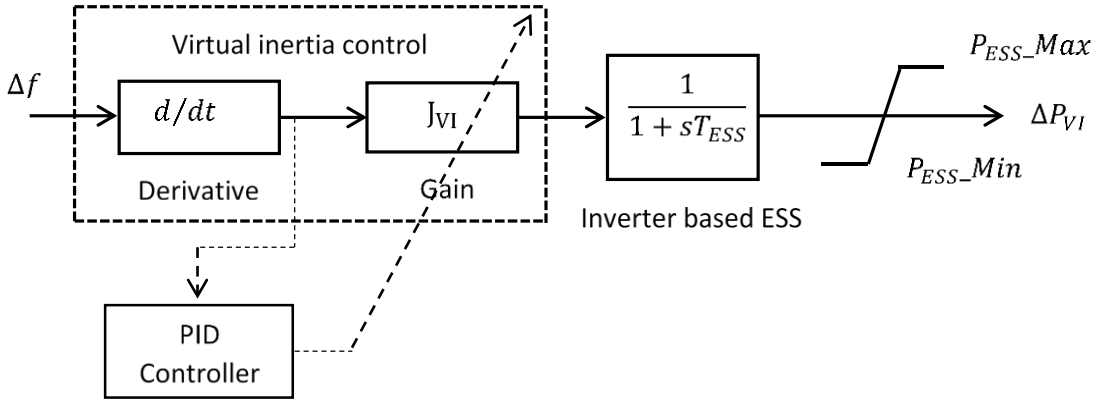

Fig. 3. Proposed PID based Virtual Inertia Controller

$$\Delta P_m(s) = \frac{1}{1+s_t}(\Delta P_g(s)) \tag{4}$$

$$\Delta P_g(s) = \frac{1}{1+sT_g}(\Delta P_c - \frac{1}{R}\Delta f(s)) \tag{5}$$

$$\Delta P_c(s) = \frac{K_i}{s}(\beta.\Delta f(s)) \tag{6}$$

$$\Delta P_W(s) = \frac{1}{1+sT_{WT}}(\Delta P_{wind}(s)) \tag{7}$$

$$\Delta P_{PV}(s) = \frac{1}{1+sT_{PV}}(\Delta P_{solar}(s)) \tag{8}$$

III. Optimal PID Controller for Virtual Inertia Control of MG

The functioning of the proposed virtual inertia control approach is such that it is independent of the main and subordinate control units while imitating the inertia property of the synchronous generator. Hence, the stored energy in the ESS is entirely used to enhance the system's frequency stability within both the steady-state and transient performance. Fig. 2 and Fig. 3 depict the modeling – in the dynamic space – of the traditional virtual inertia controller and the proposed PID-based virtual inertia approach respectively, in this paper. A derivative control technique is employed to evaluate the RoCoF for adjusting the added MG's power set point after a contingency. To eliminate the noise thereby obtaining the actual dynamic characteristics in the inverter-typed of ESS, a low-pass filter is deployed. To simulate the real ESS power response, it is required to limit the maximum/minimum ESS energy capacity, to this end, the limiter block is deployed. Consequently, the virtual inertia controller based on the optimal PID controller proposed herein, contribute to the total inertia of the MG as if the ESS has inertia characteristic comparable to the inertia property of the traditional synchronous generator, thus, improving the frequency stability as well as resilience. Equation (9) expresses the PID controller transfer function.

$$G(s) = K_p + \frac{K_i}{s} + sK_D \tag{9}$$

In equation (9), K_P, K_I and K_D denotes proportional, derivative, and integral gain respectively. In the same vein, the equation (10) expresses the control low of the proposed controller design.

$$\Delta P_{inertia} = \frac{J_{VI}}{1+sT_{Ess}}\frac{d}{dt}(\Delta f) \tag{10}$$

IV. Particle Swarm Optimization (PSO)

PSO is a population-orientated and bio-inspired optimization technique first introduced by Kennedy and Eberhart in 1995 [41]. In the conventional PSO, a bird called particle represents the solution to each optimization problem in the problem space. And objective function is used to determine the fitness values of the particles. The particles have velocities that determine the directions and distances from which they fly. This algorithm initializes a group of random particles as the initial population by random selection from the solution domain [41].

For each iteration process, the particle updates itself to find an optimal solution or approximate optimal solution using two "optimal values".

The first represents the optimal solution achieved by the particle itself. This value is termed individual optimization (pbest). The second solution, also known as global optimization (gbest) is the optimal solution achieved for the entire population. Using these two optimal values, the particles update their velocity and position according to equations (11) and (12) respectively.

$$V^{i+1} = W * V^{i} + C_1 * rand_1 * (gbest - X^{i}) + \cdots \quad (11)$$
$$C_2 * rand_2 * (pbest - X^{i})$$

$$X^{i+1} = X^{i} + V^{i+1} \quad (12)$$

$$W = W_{\min} + \frac{(t_{\max} - t)(W_{\max} - W_{\min})}{(t_{\max} - 1)} \quad (13)$$

Where v^i is the velocity of the particle i, w described in equation (13) is the inertia weight which controls the exploration and exploitation of the problem space by dynamically adjusting the particle velocity, x^i is the position of the particle i, pbest and gbest are defined as before, rand is a random number that belongs to [0, 1], C_1 and C_2 are called learning factors termed as the acceleration constants. They modify the particle velocity towards pbest and gbest, t_{max} is the maximum number of iterations and t is the current iteration. In PSO, an improved performance of the algorithm can be achieved through the appropriate selection of the inertia weight which can help to balance the global and local search ability. Different methods were employed in literature [42] to set the inertia weight, such as simulated annealing inertia weight, Gaussian, fuzzy adaptive, exponential, and parallel. However, considering both simplicity and efficiency, the inertia weight which linearly decreases is an appropriate method for determining the inertia weight. Hence, equation (13) defines the weight function, such that $w_{max} = 0.9$ and $w_{min} = 0.4$ are the values used to develop the robust PID-based virtual inertia controller.

V. Problem Formulation

Since the frequency overshoot (f_{max}), undershoot (f_{nadir}), and time taken by the frequency excursion to the desired region (t_{st}) from the nominal value, are vital features of the frequency

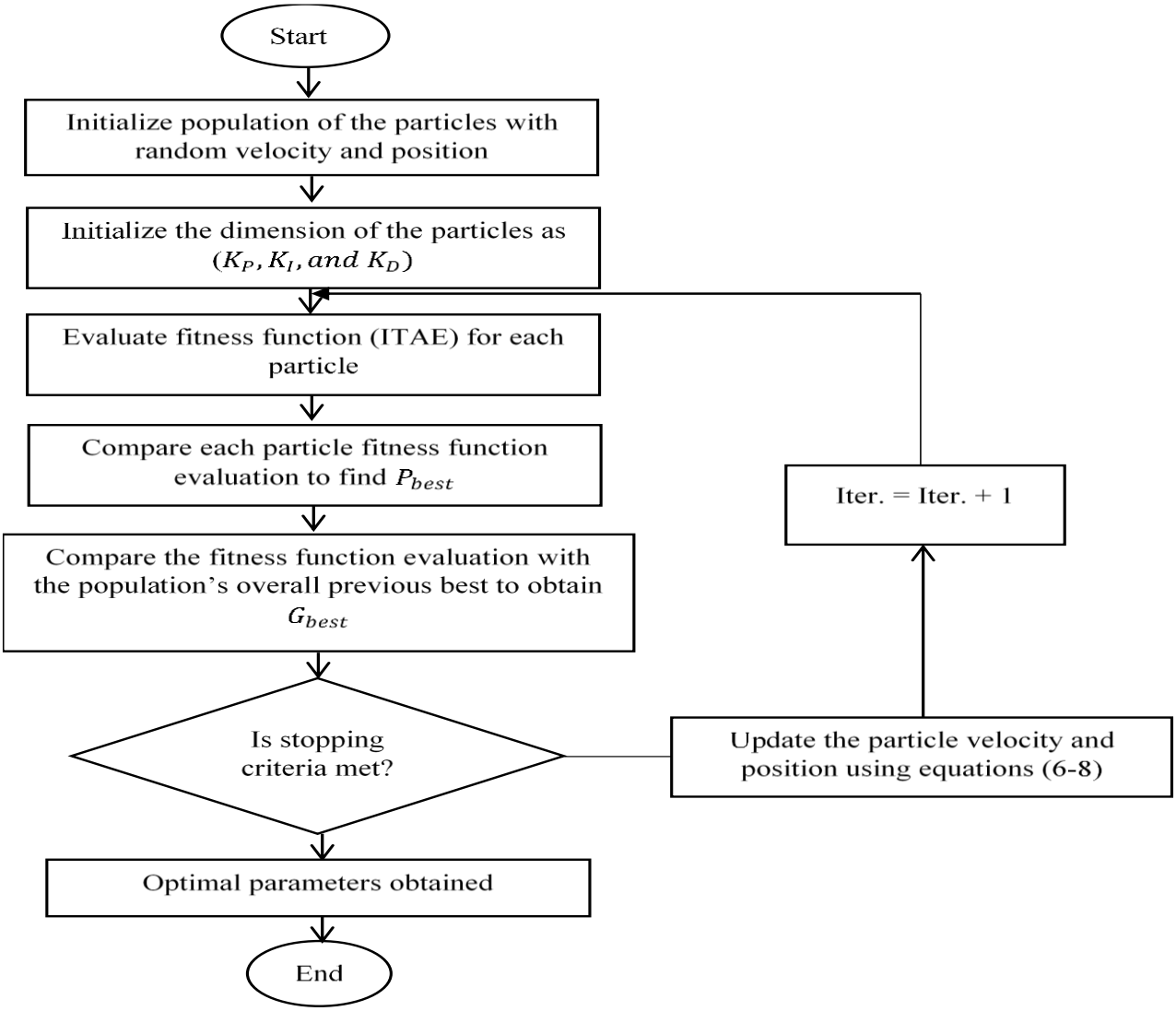

Fig.4 Flowchart of the proposed Virtual Inertia Control Based on Optimal PID Controller

response of a MG following RES penetration, these characteristics should be minimized to achieve effective frequency control. Hence, the integral of time, multiplied absolute error (ITAE) is used as objective or fitness function to find optimum values of controller parameters formulated as expressed in equation (14).

$$ISE = \int_0^{t_{sim}} |\Delta f| .t.dt \tag{14}$$

Subject to maximum and minimum values of PID controller parameters described by equation (15).

$$K_{p,i,d}^{Min} \le K_{p,i,d} \le K_{p,i,d}^{Max} \tag{15}$$

Where Δf is frequency deviation away from the nominal set point while t_{sim} is the simulation time.

The population size is chosen to consist of 20 particles, with each particle represented by a 3-dimensional vector which are the PID parameters, kp, ki, kd respectively. 50 is used as the maximum generation iteration time. The inertia weight w decreases linearly, and the inertia weight maximum and minimum are set to 0.9 and 0.4 respectively.

The proposed method is applied to obtain the optimal parameters of the PID controller by minimizing the objective function.

VI. Result and Discussion

The proposed PID-based Virtual Inertia Controller (VIC) is applied to the modern power system presented in Fig 1. Using MATLAB/Simulink software, the dynamic response model is realized. The analysis of the simulation results presented in this paper focuses on three parts. Firstly, on the frequency stability assessment of the MG under system uncertainty – nominal and reduced system inertia, 100% and 70% of H. Secondly, is the evaluation of the frequency stability assessment under degraded system inertia caused by RES penetration. Thirdly, the analysis also focuses on the evaluation of the effectiveness and robustness of the proposed PID-based virtual inertia controller design. Furthermore, the simulation results were compared with those obtained using conventional derivative based techniques and for a wide range of system operations without the VIC.

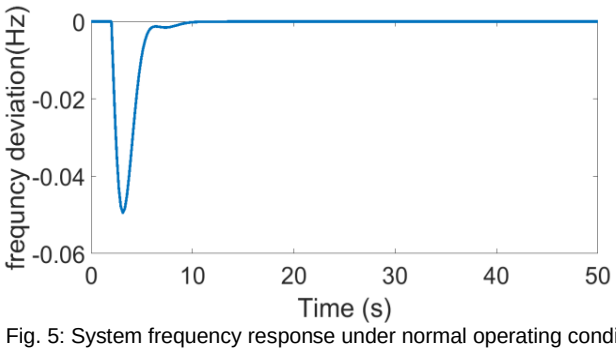

Fig. 5: System frequency response under normal operating condition of 100% system inertia without RES penetration

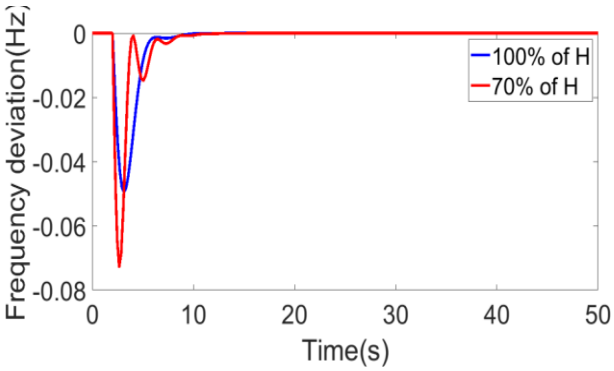

Fig. 6: Comparison of *system frequency responses under conditions of nominal and reduced system inertia without RES penetration*

Scenario 1: *Performance Analysis of the Studied Power System without RES based Power Penetration.*

Two different cases are simulated for this scenario as follows:

Case A: In this case, the performance of the test power system is carried out under the condition of the nominal system parameter such as a system with 100% system inertia. During the simulation, at a given time t=2s, a load of 0.02 p. u., is suddenly demanded and applied to the studied system. Figure 5 shows the frequency deviation for this scenario.

Case B: In this case, the frequency response of the test system evaluated under a reduced system inertia such as 70% of its value, depicting a 30% reduction. In addition, a 20% p.u., of step load change was applied to the studied system at time *t* = 2s. The frequency response for this case compared to the response in case A is shown in Fig. 6.

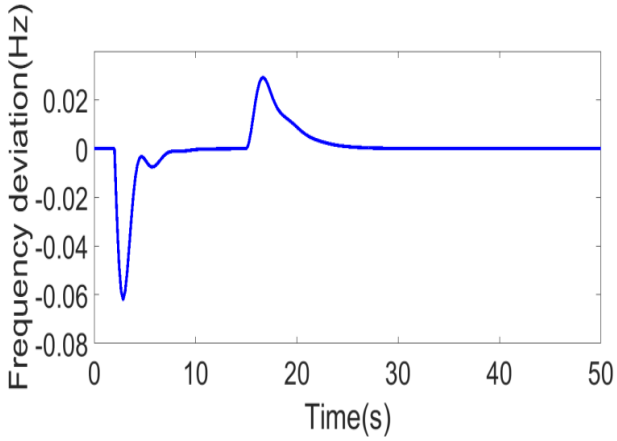

Fig. 7: *system frequency response under nominal system inertia with RES penetration*

In Fig.6 observe that the low system inertia condition negatively affects the system performance and stability which results in a huge increase in the frequency nadir. Compared to the frequency response of the nominal system inertia value which is 100% of H, depicted in Fig.5, the frequency nadir significantly increases to -0.073Hz from -0.049 as illustrated by the red line curve in Fig.6. The increase is about 48.98%. This scenario can result in system collapse due to cascading outages if no control scheme is provided within the specified timescale. Moreover, with increased inverter-based RES penetration, this problem can be exacerbated. This possibility is demonstrated next and analyzed in scenario 2.

Scenario 2: *Performance Analysis in the Presence of RES-based Power Penetration.*

This scenario is divided into two sub-scenarios:

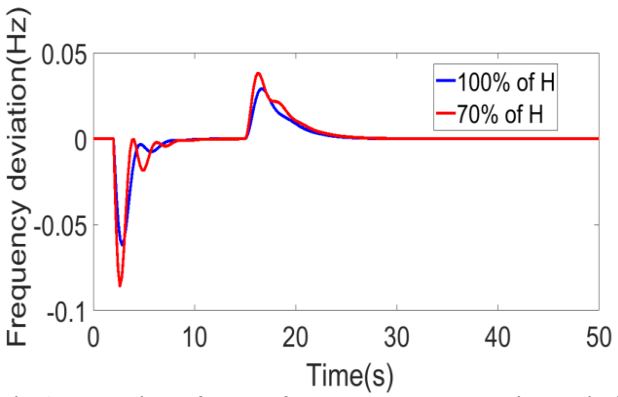

Fig. 8: *comparison of system frequency responses under nominal and reduced system inertia with RES penetration*

Case A: The islanded MG system, in this case, is analyzed considering 100% of default system inertia and multiple disturbances comprising of 20% p.u step load change at time t = 2 s and swift rise in solar and wind power (both of 0.01p.u.) at 15 s. Fig. 7 depicts the frequency response under this case.

AS depicted in Fig.7, the critical inertia decrease due to increased RESs penetration deteriorates the frequency stability and the system resiliency. The sudden huge frequency rise (overshot) +0.03Hz and increase in the frequency nadir with longer stabilizing time also substantiate that RES penetration adversely affects the frequency stability. Compared to the system response of Fig.5 before the sudden RES injection, the frequency nadir significantly increases to -0.062Hz from -0.049 and overshot rises to +0.03Hz. The increase is about 26.53%.

Case B: Under this illustration, the MG is studied and analyzed with reduced inertia of 70% from its nominal value with the application of multiple disturbances such as 20% p.u incremental load change at time t = 2 s as well as a sudden rise in solar and wind power (both of 0.01p.u.) occurring at 15 s. The system response in terms of frequency compared to the response in Case A is depicted in Fig. 8.

From Fig. 8, observe that due to the reduction in the system inertia from 100% to 70% and further inertia degradation caused by RES penetration, the system frequency stability was negatively impacted. Compared with the system response under the condition of system nominal inertia of 100% displayed by the blue line curve in Fig. 8, a huge frequency rise (overshoot) from +0.029 to +0.038 and an increase in the frequency nadir (undershoot) from –0.062 to –0.086 were observed as displayed by the red line in Fig.8, hence, the deterioration of the system frequency stability and this may lead to the tripping of the generation, load shedding and may results in collapse of the system and power blackouts. To preserve the dynamic security of the system, the proposed PID-based VIC is applied in the next scenario.

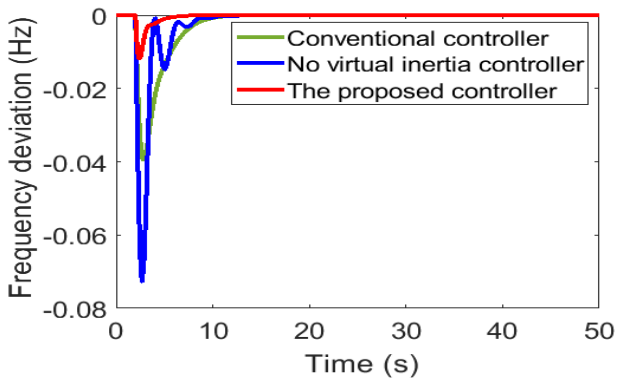

Fig. 9 System frequency response of the PID-based VIC and conventional VIC under low system inertia condition

Scenario 3: *Performance evaluation of the proposed controller*

Two different cases simulated for this scenario are presented as follows:

Case A: In this case, the optimally designed PSO based-PID controller is tested on the studied power system with the introduced uncertainty (i.e. 70% of H) without RES penetration. Also, a disturbance representing a 0.02 p.u. change in load is applied. Fig.9 presents the combined system frequency response consisting of the VIC-based optimal PID controller, conventional VIC, and the case without VIC.

As can be observed from Fig. 9, the system response in terms of frequency without any control strategy oscillates outside the permissible frequency range due to change in step load of 0.02p.u., as depicted by the blue line curve. By deploying the VIC based on conventional approach, the frequency nadir reduces to -0.039 Hz from -0.073 Hz. Upon deployment of the VIC-based optimal PID controller, an enhancement of system frequency stability is obtained, with further reduction in the frequency nadir to -0.012 Hz observed as depicted by the red line curve. The reduction amount to about 69.2% compared to conventional VIC. This, therefore, depicts the superiority in performance of the proposed controller compared with the conventional VIC.

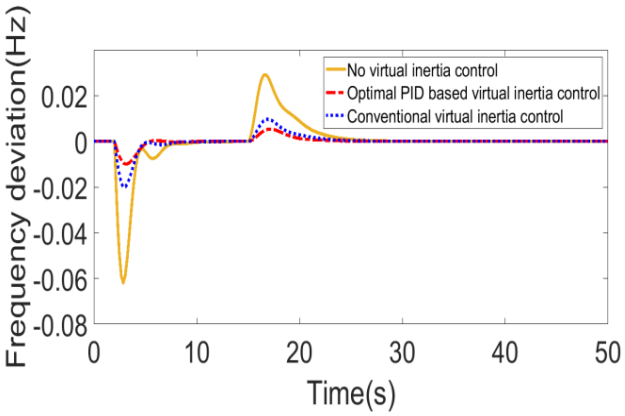

Fig. 10 System response in terms of frequency of the PID based virtual inertia controller and conventional virtual inertia controller under nominal system inertia condition and RESs integration

Case B: Here, the performance of the optimally designed PSO based-PID controller is tested on the studied power system with nominal system inertia (i.e. 100% of H) and multiple disturbances of 20% p.u load change at time t = 2 s and swift rise in solar and wind power (both of 0.01p.u.) applied at 15 s. Fig. 10 shows the system frequency response under the. VIC-based optimal PID controller, conventional VIC, and without VIC.

As observed from Fig. 10, the proposed VIC-based optimal PID controller successfully mitigates the frequency deviation thereby guaranteeing an improved and robust performance when paralleled with or without the VIC. By implementing the conventional VIC, the nadir and overshoot in frequency drastically decrease to -0.02 Hz from –0.062 and +0.01 Hz from +0.029 respectively as depicted by the blue line curve. This reduction is about 67.7% and 50% respectively. However, further improvement in the reduction of the frequency nadir and overshoot to -0.009Hz and +0.005Hz respectively, were observed upon deployment of the VIC-based optimal PID controller which is designed optimally using the PSO algorithm. These represent 50.7% and 44.4% respectively when compared to the studied system with the conventional VIC. The optimum PID gains of the controller obtained are given in Table II.

TABLE II
OPTIMUM VALUE OF THE PID CONTROLLER PARAMETERS

	K_P	K_I	K_D
PSO TUNED PID CONTROLLER	2.107	9.116	0.036

This proves that the VIC-based optimal PID controller could reasonably provide an optimally suitable value of virtual inertia constant. Hence, the PID-based VIC system designed using PSO technique can achieve quite better improved frequency stability under a wide range of disturbances and system uncertainty. And this helps to corroborate the effectiveness and robustness of the designed controller for maintaining the system dynamic security.

VII. CONCLUSION

Increased deployment of power electronic based RES generators characterized the modern power system, which has the potential of causing stability problems due to their distinctive characteristics. To minimize the undesirable effects, herein this work developed a frequency control scheme using PID-typed VIC for enhancing system inertia and frequency stability. Derivative control method is employed for the control of inverter-based ESS for inertia synthesis of a studied MG. In achieving optimal performance, the PID controller parameters are optimize using PSO algorithm. A demonstration under several scenarios reveal the stabilizing and enhanced performance of the PID-based VIC under a wide range of system disturbances and uncertainties. It is also deduced that increased RESs penetration result in low system inertia, while in the situation where no inertia controller, the control units is unable to regulate frequency oscillations within a tolerable range due to the absence of virtual emulation and ultimately leading to system instability. By employing the conventional VIC, a reduction in both the frequency nadir and overshoot was observed. However, significant reduction in both frequency nadir and overshoot was observed in the case of the PID-based VIC controller proposed in this paper, as compared with Other VICs. The reductions were observed to be 50.7% and 44.4% respectively. Similarly, under the situation of system uncertainty, 70% of H, an improvement in the performance with the PID-based VIC proposed controller, against the conventional VIC indicates a 69.2% improvement in the reduction of frequency nadir. This clearly helps to validate the superior and robust capability of the proposed PID-based VIC technique under varied system conditions and uncertainties.

REFERENCES

[1] M. Dreidy, H. Mokhlis, S. Mekhilef, “Inertia response and frequency control techniques for renewable energy sources: A review”, Renew. Sustain. Energy Rev., vol. 69 no. 1, pp. 144–155, 2017, DOI: 10.1016/j.rser.2016.11.170.

[2] Y. Liu, S. You, J. Tan, Y. Zhang, and Y. Liu, “Frequency response assessment and enhancement of the U.S. power grids towards extra-high photovoltaic generation penetrations – an industry perspective,” IEEE Trans. Power Sys., vol. 33, no. 3, pp. 3438–3449, Jan. 2018.

[3] International review of frequency control adaptation, Australia Energy Market Operator. Melbourne, VIC, Australia, 2017. [Online]. Available: http://www.aemo.com.au.

[4] RoCoF Modification Proposal – TSOs’ Recommendations, EirGrid/SONI, Ballsbridge, DUB, Ireland, Sep. 4, 2012.

[5] P. P. Zarina, S. Mishra, and P. C. Sekhar, “Deriving inertial response from a non-inertial PV system for frequency regulation,” in Proc. IEEE PEDES, pp. 1–5, Bengaluru, India, 16−19 Dec. 2012.

[6] N. Kakimoto, S. Takayama, H. Satoh, and K. Nakamura, “Power modulation of photovoltaic generator for frequency control of power system,” IEEE Trans. Energy Convers., vol. 24, no. 4, pp. 943–949, Dec. 2009.

[7] A. F. Hoke, M. Shirazi, S. Chakraborty, E. Muljadi, and D. Maksimovic, “Rapid active power control of photovoltaic systems for grid frequency support,” IEEE J. Emerg. Sel. Topics Power Electron., vol. 5, no. 3, pp. 1154–1163, Sep. 2017.

[8] E. Spahic, D. Varma, G. Beck, G. Kuhn, and V. Hild, "Impact of reduced system inertia on stable power system operation and an overview of possible solutions", in *Proc. PESGM*, Boston, MA, USA, 17–21 Jul.2016.

[9] Z. Chen, J. M. Guerrero, and F. Blaabjerg, “A review of the state of the art of power electronics for wind turbines,” IEEE Trans. Power Electron., vol. 24, no. 8, pp. 1859–1875, Aug. 2009.

[10] J. Morren, S. W. H. de Haan, W. L. Kling, and J. A. Ferreira, “Wind turbines emulating inertia and supporting primary frequency control,” IEEE Trans. Power Sys., vol. 21, no. 1, pp. 433–434, Feb. 2006.

[11] L. Holdsworth, J. Ekanayake, and N. Jenkins, “Power system frequency response from fixed speed and doubly fed induction generator based wind turbines,” Wind Energy, vol. 7, pp. 21–35, 2004.

[12] A. Mullane and M. O’Malley, “The inertial response of induction-machine-based wind turbines,” IEEE Trans. Power Sys., vol. 20, no. 3, pp. 1496–1503, Aug. 2005.

[13] J. Ekanayake, and N. Jenkins, “Comparison of the response of doubly fed and fixed-speed induction generator wind turbines to changes in network frequency,” IEEE Trans. Energy Conv., vol. 19, no. 4, pp. 800−802, Dec. 2004.

[14] G. Lalor, A. Mullane, and M. O’Malley, “Frequency control and wind turbine technologies,” IEEE Trans. Power Sys., vol. 20, no. 4, pp. 1905–1913, Nov. 2005.

[15] F. Blaabjerg and K. Ma, “Future on power electronics for wind turbine systems,” IEEE J. Emerg. Sel. Topics Power Electron., vol. 1, no. 3, pp. 139–152, Sep. 2013.

[16] M. Kayikçi and J. V. Milanovic, “Dynamic contribution of DFIG-based wind plants to system frequency disturbances,” IEEE Trans. Power Sys., vol. 24, no. 2, pp. 859–867, May 2009.

[17] J. F. Conroy and R. Watson, “Frequency response capability of full converter wind turbine generators in comparison to conventional generation,” IEEE Trans. Power Sys., vol. 23, no. 2, pp. 649–656, May 2008, DOI: 10.1109/TPWRS.2008.920197.

[18] K. Liu, Y. Qu, H. Kim, and H. Song, “Avoiding frequency second dip in power unreserved control during wind power rotational speed recovery,” IEEE Trans. Power Sys., vol. 33, no. 3 pp. 3097-3106, May 2018, DOI: 10.1109/TPWRS.2017.2761897.

[19] M. Arani and E. Saadany, “Implementing virtual inertia in DFIG-based wind power generation,” IEEE Trans. Power System, vol. 28, no. 2, pp. 1373-1384, May 2013, ODI: 10.1109/TPWRS.2012.2207972.
[20] L. Miao, J. Wen, H. Xie, C. Yue, and W. Lee, "Coordinated control strategy of wind turbine generator and energy storage equipment for frequency support", IEEE Trans. Ind. Appli., vol. 51, no. 4, pp. 2732-2742, July-Aug. 2015, doi: 10.1109/TIA.2015.2394435.
[21] M. F. M. Arani and Y. A. -R. I. Mohamed, "Analysis and Damping of Mechanical Resonance of Wind Power Generators Contributing to Frequency Regulation," in IEEE Transactions on Power Systems, vol. 32, no. 4, pp. 3195-3204, July 2017, DOI: 10.1109/TPWRS.2016.2618391
[22] H.-P. Beck and R. Hesse, ``Virtual synchronous machine," in Proc. 9th Int. Conf. Elect. Power Qual. Utilisation (EPQU), Oct. 2007, pp. 1-6.
[23] Y. Chen, R. Hesse, D. Turschner, and H.-P. Beck, ``Improving the grid power quality using virtual synchronous machines," in Proc. Int. Conf. Power Eng. Energy Elect. Drives, May 2011, pp. 1-6.
[24] Y. Chen, R. Hesse, D. Turschner, and H.-P. Beck, ``Investigation of the virtual synchronous machine in the island mode," in Proc. IEEE PES Innov. Smart Grid Technol. Conf. Eur., Oct. 2012, pp. 1-6.
[25] J. Driesen and K.Visscher, ``Virtual synchronous generators," in Proc. 21st IEEE Power Energy Soc. Gen. Meeting, Convers. Del. Elect. Energy (PES), Jul. 2008, pp. 1-3.
[26] H. Bevrani, T. Ise, and Y. Miura, ``Virtual synchronous generators: A survey and new perspectives," Int. J. Electr. Power Energy Syst., vol. 54, pp. 244_254, Jan. 2014.
[27]. H. Gu, R. Yan, T.K. Saha, Minimum synchronous inertia requirement of renewable power
systems. IEEE Trans. Power Syst. **33**(2), 1533–1543 (2018).
[28] S. D'Arco, J. A. Suul, and O. B. Fosso, ``A virtual synchronous machine implementation for distributed control of power converters in smartgrids," Electr. Power Syst. Res., vol. 122, pp. 180_197, May 2015.
[29] Q.-C. Zhong and G. Weiss, ``Synchronverters: Inverters that mimic synchronous generators," IEEE Trans. Ind. Electron., vol. 58, no. 4, pp. 1259_1267, Apr. 2011.
[30] U. Tamrakar, D. Shrestha, M. Maharjan, B. P. Bhattarai, T. M. Hansen, and R. Tonkoski, ``Virtual inertia: Current trends and future directions," Appl.Sci., vol. 7, no. 7, p. 654, 2017.
[31] E. Rakhshani, D. Remon, A. M. Cantarellas, J. M. Garcia, and P. Rodriguez, ``Virtual synchronous power strategy for multiple HVDC interconnections of multi-area AGC power systems," IEEE Trans. Power Syst., vol. 32, no. 3, pp. 1665_1677, May 2017.
[32] E. Rakhshani, D. Remon, A. M. Cantarellas, and P. Rodriguez, ``Analysis of derivative control based virtual inertia in multi-area high-voltage direct current interconnected power systems," IET Gener. Transmiss. Distrib., vol. 10, no. 6, pp. 1458_1469, Apr. 2016.
[33] E. Rakhshani and P. Rodriguez, ``Inertia emulation in AC/DC interconnected power systems using derivative technique considering frequency measurement effects," IEEE Trans. Power Syst., vol. 32, no. 5, pp. 3338_3351, Sep. 2017.
control of grid-scale BESS on power system frequency response," in Proc.Int. Conf. Students Appl. Eng. (ICSAE), Oct. 2016, pp. 254_258.
[34] T. Kerdphol, F. S. Rahman, Y. Mitani, K. Hongesombut, and S. Küfeo_glu, ``Virtual inertia control-based model predictive control for micro-grid frequency stabilization considering high renewable energy integration," Sustainability, vol. 9, no. 5, p. 773, 2017.
[35] T. Kerdphol, F. S. Rahman, Y. Mitani, M. Watanabe, and S. Küfeoglu, ``Robust virtual inertia control of an islanded micro-grid considering high penetration of renewable energy," IEEE Access, vol. 6, pp. 625_636, 2017.
[36] H. Bevrani, M. R. Feizi, and S. Ataee, ``Robust frequency control in an islanded micro-grid:$H_\infty$and μ-synthesis approaches," IEEE Trans. Smart Grid, vol. 7, no. 2, pp. 706_717, Mar. 2016.
[37] Mentesidi, K., Garde, R., Agudo, M., et al.: ‘Implementation of a fuzzy logic controller for virtual inertia emulation’. IEEE Conf., Smart Electrical Distribution System and Technology, Vienna, Austria, 2015, pp. 606–611
[38] Hu, Y., Wei, W., Peng, Y., et al.: ‘Fuzzy virtual inertia control for virtual synchronous generator’. IEEE Conf., 35th Chinese Control Conf., Chengdu,
China, 2016, pp. 1–6
[39] H. Bevrani, *Robust Power System Frequency Control*, 2nd ed. New York, NY, USA: Springer, 2014.
[40] M. H. Fini and M. E. H. Golshan, ``Determining optimal virtual inertia and frequency control parameters to preserve the frequency stability in islanded micro-grids with high penetration of renewables," *Electr. Power Syst. Res.*, vol. 154, no. 1, pp. 13_22, 2018.
[41] Poli R., Kennedy J., Blackwell T. ‘Particle swarm optimization an overview’. *Swarm Intelligence.* 2007; 1:33–57
[42] Jordehi A.R., Jasni J. ‘Parameter selection on particle swarm optimization: a survey’. *Journal of Experimental & Theoretical Artificial Intelligence*. 2013:25(4):527–42